Structure in the giant resonance region of ^{16}O observed with the reaction ^{13}C(^{3}He,γ)^{16}O

E. Ventura

Department of Physics, Stanford University, Stanford, California 94305
and Departmento de Física, Comision Nacional de Energia Atomica, Buenos Aires, Argentina

J. R. Calarco, C. C. Chang,* E. M. Diener,† D. G. Mavis, and S. S. Hanna

Department of Physics, Stanford University, Stanford, California 94305

G. A. Fisher

Department of Physics, Stanford University, Stanford, California 94305
and Department of Physics, San Francisco State University, San Francisco, California 94132

The capture reaction ^{13}C(^{3}He,γ)^{16}O has been studied over an excitation energy range of 25 to 30 MeV in ^{16}O. The 90° differential yield curve for the ground state transition shows resonances at $E_x = 25.1$, 26.0 and 27.3 MeV. The measured angular distributions are consistent with a spin and parity assignment of $J^\pi = 1-$ to these states. The relation between this structure and that observed in the ^{15}N(p,γ_0)^{16}O reaction is discussed. The 90° differential yield curves for the doublet transitions $\gamma_1 + \gamma_2$ and $\gamma_3 + \gamma_4$ were also measured. The former shows resonances at $E_x = 26.0$, 26.6, 27.2, 27.7, and 28.6 MeV, while the latter shows a broad resonance centered at $E_x \simeq 27.5$ MeV with mild structure. Both curves suggest the existence of giant resonance strength built on the excited states of ^{16}O.

> NUCLEAR REACTIONS ^{13}C(^{3}He,γ)^{16}O, $E_{3_{He}} = 3.0$-8.5 MeV, measured $\sigma(E_{3_{He}}, E_\gamma, \theta)$. ^{16}O deduced resonances and structure in giant resonance region. Enriched ^{13}C target.

I. INTRODUCTION

The giant E1 resonance in ^{16}O has been extensively studied both theoretically and experimentally. The simple particle-hole model explains the dominant features of the E1 strength, but prominent details are not yet fully understood. Progress toward understanding the intermediate structure was made by observations, both theoretical[1] and experimental,[2] that the structure could be associated with n-particle--n-hole configurations. Recently, this interpretation has been greatly strengthened by observations with the reaction ^{15}N($\vec{p},\gamma_0$)^{16}O.[3]

The work of Shakin and Wang[4] on coupling of 3p-3h states to the basic 1p-1h states obtained excellent agreement with the structure observed throughout the E1 resonance in a 1p-1h reaction such as the (γ,n_0) process. It is therefore of interest to look for 3p-3h states which might be expected to appear in the capture reaction ^{13}C(^{3}He,γ_0)^{16}O. In experiments below E(^{3}He) = 3.5 MeV structure has indeed been observed[5] in a region in ^{16}O where significant intermediate structure appears in the reaction ^{15}N(p,γ_0)^{16}O. The present experiment extends the observations on the reaction ^{13}C(^{3}He,γ_0)^{16}O to E(^{3}He) = 8.5 MeV, which corresponds to an excitation energy of 30 MeV in ^{16}O.

Since our observations were first reported,[6] Shay et al.[7] have measured the ^{13}C(^{3}He,γ_0)^{16}O yield up to an excitation energy of 35 MeV in ^{16}O. These authors have also obtained information on the transitions to the lowest four excited states in ^{16}O. However, they were unable to resolve the individual transitions in that group. Our measurements were able to resolve the transitions to the first and second excited states ($\gamma_1 + \gamma_2$) from those to the third and fourth excited states ($\gamma_3 + \gamma_4$). The measured yield curves for these doublet transitions revealed structure not observed in the work of Shay et al.[7] The gross structures in these curves strongly indicate the presence of giant dipole resonance strength built on the low excited states of ^{16}O.

II. EXPERIMENTAL PROCEDURE

The Stanford FN tandem Van de Graaff accelerator provided ^{3}He$^+$ beams over the energy range E(^{3}He) = 3.0-8.5 MeV. Gamma rays were detected with a 24 cm x 24 cm NaI(Tℓ) crystal surrounded by a plastic scintillator operated in anticoincidence.[8]

Fairly thick (100-300 μg/cm^2) self-supporting targets of ^{13}C were made by cracking methane (CH$_4$) enriched to 95% in ^{13}C. Briefly, the method consisted in heating a 0.001 cm thick tantalum foil (2.5 cm wide × 10 cm long) to approximately 2500° C in vacuum and then introducing the CH$_4$ gas into the evacuated bell jar until the pressure reached approximately 1/3 atm. The tantalum foil with carbon deposited on both sides was then removed and allowed to cool. Owing to the difference in the co-
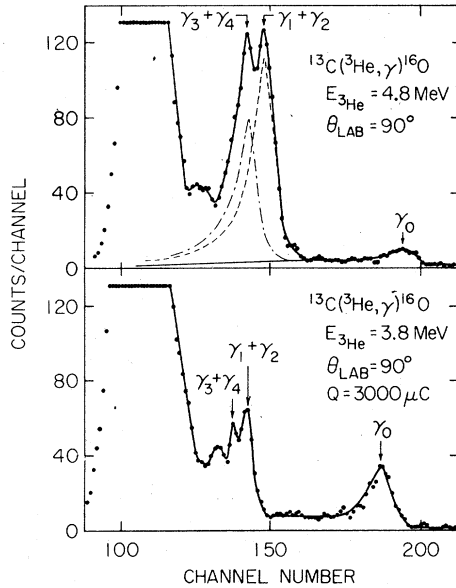
FIG. 1. Gamma ray spectra from the bombardment of an enriched ^{13}C target by ^{3}He ions at $E(^3He) = 3.8$ and 4.8 MeV. Transitions to the ground and first four excited states in ^{16}O are seen. The transitions to the 6.052 and 6.131 MeV states (labeled $\gamma_1 + \gamma_2$) are resolved from those to the 6.917 and 7.119 MeV states (labeled $\gamma_3 + \gamma_4$). In the top spectrum the decomposition into two groups is shown.

efficients of expansion of tantalum and carbon, this cooling process allowed an easy removal of the carbon foil for subsequent mounting.

Gamma ray spectra were recorded at intervals of 200 keV in the bombarding energy. The detector was placed at an angle of 90° with respect to the beam. Figure 1 shows typical spectra taken at $E(^3He) = 3.8$ and 4.8 MeV. Capture radiations to the ground and first four excited states in ^{16}O are seen. However, the NaI detector could not resolve transitions to the 6.05 and 6.13 MeV states (labeled $\gamma_1 + \gamma_2$) nor the transitions to the 6.92 and 7.12 MeV states (labeled $\gamma_3 + \gamma_4$). The resolution of these two groups from the background improves considerably at higher bombarding energies because the peaks move further away from the large stationary peak caused by the reaction ^{13}C(^{3}He,$\alpha\gamma_{15.1}$)^{12}C. The data were analyzed by use of a computer program which fits, by the method of least squares, the correct γ-ray line shapes to the observed peaks. Only three lines were used: one for γ_0 and one each for $\gamma_1 + \gamma_2$ and $\gamma_3 + \gamma_4$.

The absolute differential cross section at 90° for ^{13}C(^{3}He,γ_0)^{16}O was determined from an accurate measurement of the target thickness using Rutherford scattering of 1.0 MeV ^{3}He ions. The value obtained at $E(^3He) = 4.0$ MeV is $d\sigma(90°)/d\Omega = 0.67 \pm 0.12$ µb/sr. Another value for the absolute
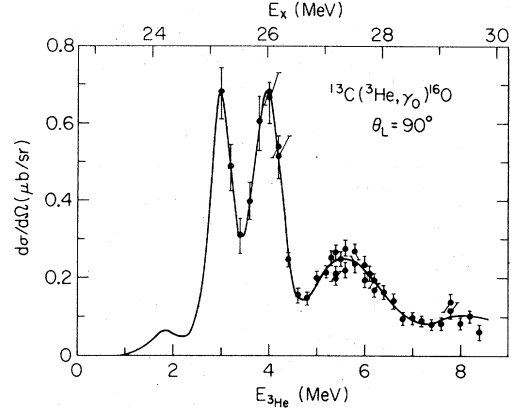

FIG. 2. Excitation function of the differential cross section for ^{13}C(^{3}He,γ_0)^{16}O at $\theta_{lab} = 90°$. The data up to $E(^3He) = 3.0$ MeV are taken from Ref. 5 and normalized to the present work at $E(^3He) = 3.0$ MeV.

differential cross section of ^{13}C(^{3}He,γ_0)^{16}O was determined by comparing its yield to the yield of the 15.1 MeV gamma rays from the reaction ^{13}C(^{3}He,$\alpha\gamma_{15.1}$)^{12}C, whose cross section is known to an accuracy of 30%.[9] The value obtained this way at $E(^3He) = 4.0$ MeV is $d\sigma(90°)/d\Omega = 0.58 \pm 0.19$ µb/sr. The value obtained in the first method is the one adopted with an overall error of ±20%. From it the absolute differential cross sections for the other groups were deduced.

III. RESULTS AND DISCUSSION

A. Capture to the ground state

The 90° excitation function for the reaction ^{13}C(^{3}He,γ_0)^{16}O is shown in Fig. 2 joined with the curve of Puttaswamy and Kohler.[5] In addition to the two resonances at $E(^3He) = 1.8$ and 3.0 MeV seen by Puttaswamy and Kohler, two more resonances at $E(^3He) = 4.0 \pm 0.1$ and 5.6 ± 0.1 are observed. These four resonances correspond to states in ^{16}O at $E_x = 24.05 \pm 0.10$, 25.12 ± 0.05, 26.0 ± 0.1 and 27.3 ± 0.2 MeV, respectively. These measurements are in excellent agreement with Ref. 7 regarding the shape of the excitation function. However, the magnitude of the 90° absolute differential cross section measured by Shay et al.[7] is approximately 30% lower than the one measured in the present work, but the difference is within the combined errors.

Angular distributions taken at $E(^3He) = 3.4, 3.8, 4.0, 4.7, 5.5$ and 6.7 MeV are shown in Fig. 3. A thick (≈ 300 µg/cm^2) ^{13}C target was used for this purpose, and the energy loss of the ^{3}He ions passing through this foil was taken into account in determining the bombarding energy. The measured angular distributions were fitted to the expression

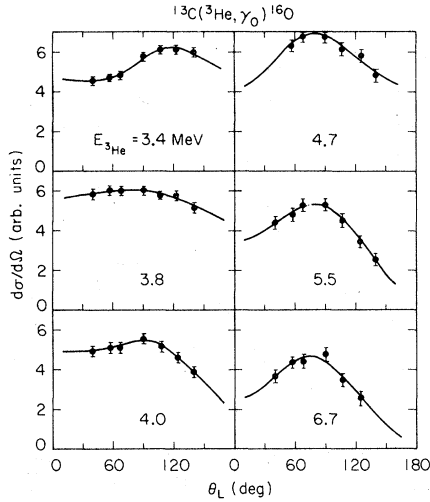$$W(\theta) = A_0 \left[1 + \sum_{1}^{3} a_k P_k(\cos\theta) \right]. \quad (1)$$

FIG. 3. Angular distributions for the ^{13}C(^{3}He,γ_0)^{16}O reaction. The curves are least squares fits of Eq. (1) with $k = 1 \rightarrow 3$.

The results of these fits are shown in Table I. The angular distributions on resonance show a pattern that is characteristic of giant E1 resonances in many nuclei. Therefore, one may identify the states observed in this reaction as characteristic $J^{\pi} = 1^{-}$ dipole states in ^{16}O.

In Fig. 4 we have plotted the values of the a_k coefficients extracted from the measured angular distributions, together with the values obtained by Shay et al.[7] The a_1 coefficient possibly fluctuates somewhat but has an overall variation from a negative value at low energy to a positive value at the higher energies. The a_2 coefficient varies rather smoothly with energy from about zero at the lower bombarding energies to about -0.5 at $E_x = 26.5$ MeV and then seems to remain constant for a few more MeV. The a_3 coefficient is small throughout the entire region.

Assuming only E1 radiation we can pass from the quantities A_0 and a_2 to the amplitudes in the entrance channel in the j representation of the reaction ^{13}C(^{3}He,γ_0)^{16}O. Only incident waves with ($\ell = 0$, $j = 1/2$)
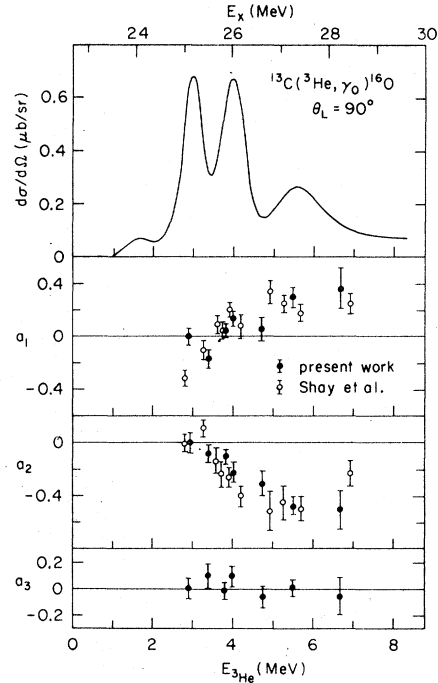

FIG. 4. Top: excitation function for the reaction ^{13}C(^{3}He,γ_0)^{16}O at $\theta_{\text{lab}} = 90°$. Bottom: the angular distribution coefficients a_k plotted against energy.

and ($\ell = 2$, $j = 3/2$) can combine with the $1/2^{-}$ ground state of ^{13}C to form a $J^{\pi} = 1^{-}$ state in ^{16}O. Thus for E1 radiation we have the transition scheme $1/2^{-}(s_{1/2},d_{3/2})1^{-}(E1)0^{+}$ which determines the angular distribution. The corresponding T-matrix elements may be written as

$$s_{1/2}e^{i\phi_s} \quad \text{and} \quad d_{3/2}e^{i\phi_d},$$

where $s_{1/2}$ and $d_{3/2}$ are the real amplitudes and ϕ_s and ϕ_d the real phases. Neglecting all radiations except E1 we obtain

$$a_2 = -0.5(d_{3/2})^2$$
$$+ 1.414(s_{1/2})(d_{3/2})\cos(\phi_d - \phi_s), \quad (2)$$

TABLE I. Angular distributions in ^{13}C(^{3}He,γ_0)^{16}O as determined from the data of Fig. 3 and a measurement at 2.9 MeV.

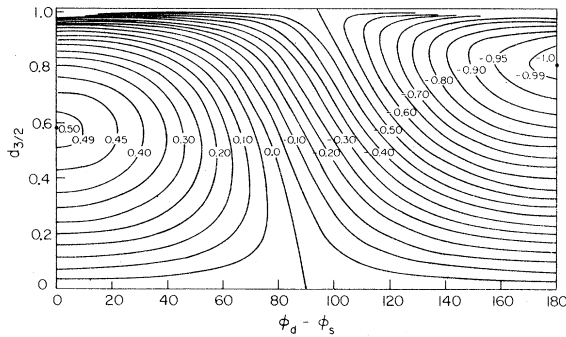| $E_{^3He}$ (MeV)	E_x (MeV)	$W(\theta)$		
		a_1	a_2	a_3
2.9	25.1	$\simeq 0$	$\simeq 0$	$\simeq 0$
3.4	25.5	-0.16 ± 0.03	-0.08 ± 0.04	0.12 ± 0.05
3.8	25.9	0.06 ± 0.02	-0.09 ± 0.02	0.01 ± 0.03
4.0	26.0	0.15 ± 0.03	-0.24 ± 0.04	0.10 ± 0.05
4.7	26.6	0.05 ± 0.07	-0.27 ± 0.08	-0.06 ± 0.09
5.5	27.3	0.30 ± 0.04	-0.49 ± 0.06	0.02 ± 0.08
6.7	28.1	0.37 ± 0.13	-0.56 ± 0.14	-0.08 ± 0.15

FIG. 5. Allowed values of the $d_{3/2}$ amplitude as a function of the phase difference $\phi_d - \phi_s$ for different values of the angular distribution coefficient a_2 in the reaction $^{13}C(^{3}He,\gamma_0)^{16}O$. The $d_{3/2}$ amplitudes are normalized as in Eq. (3).

$$A_0 = (s_{1/2})^2 + (d_{3/2})^2 = 1. \qquad (3)$$

This normalization eliminates A_0 from further consideration.

Since these two equations in three unknowns ($s_{1/2}$, $d_{3/2}$, $\phi_d-\phi_s$) cannot yield unique solutions, we have plotted in Fig. 5 the allowed variation of the $d_{3/2}$ wave against the phase difference ($\phi_d-\phi_s$) for different values of a_2. These curves show that it is possible to go from a predominantly $s_{1/2}$ configuration at low energy to a predominantly $d_{3/2}$ configuration at higher energy as a_2 changes from 0 to -0.5 (see Fig. 5) with the phase difference restricted to variations between 80° and 100°. A shift from s to d wave capture is consistent with the interpretation that as we go to the higher bombarding energies the $d_{3/2}$ wave, originally suppressed by small penetrability, starts to dominate the reaction process.

In the above discussion we have neglected the possible presence of M1 or E2 strength. The observation of a strong trend in the a_1 coefficient is, however, indicative of strong M1-E1 or E2-E1 interference. From the fact that the a_4 coefficient remains very small we may conclude that if the trend in a_1 is produced by E2-E1 interference, the E1 radiation dominates the E2 radiation. On the other hand, it is not possible to establish the dominance of E1 over M1 radiation solely on the basis of the angular distributions or arguments based on permissible E1 and M1 radiation widths. However, the M1 strength is expected to be very small because of the closed shell nature of ^{16}O and only an unexpected preference for M1 strength in the $(^{3}He,\gamma)$ reaction would make it possible for M1 strength to compete successfully with E1 strength.

It is now interesting to compare the structures observed in the $^{13}C(^{3}He,\gamma_0)^{16}O$ reaction, the $^{14}N(d,\gamma_0)^{16}O$ reaction,[2] and the $^{12}C(\alpha,\gamma_0)^{16}O$ reaction[10] with those observed in the $^{15}N(p,\gamma_0)^{16}O$ reaction,[11] as shown in Fig. 6. We note that resonances seen in (α,γ) and (d,γ) and the two
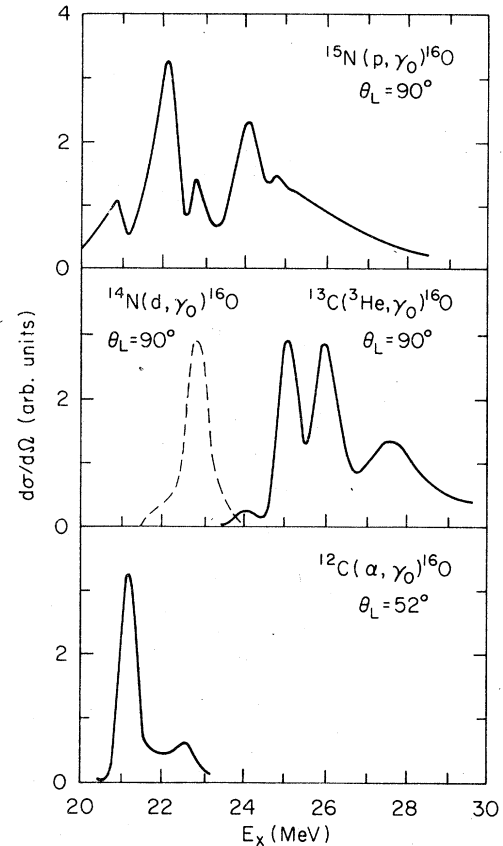
FIG. 6. Comparison of the reactions $^{13}C(^{3}He,\gamma_0)^{16}O$, $^{15}N(p,\gamma_0)^{16}O$ (Ref. 11), $^{14}N(d,\gamma_0)^{16}O$ (Ref. 2) and $^{12}C(\alpha,\gamma_0)^{16}O$ (Ref. 10).

lower resonances in $(^{3}He,\gamma)$ appear in a region where significant structure is observed in the (p,γ) reaction. However, the two upper resonances in $(^{3}He,\gamma)$ fall in a region where the (p,γ) yield is relatively smooth. This behavior perhaps indicates that the high energy tail in the (p,γ) strength is of a different character from the lower 1p-1h states and does not interfere noticeably with the 3p-3h states excited by $(^{3}He,\gamma)$.

The model of important 3p-3h components interfering with the main structure of the giant resonance was used by Shakin and Wang[4] to obtain very good agreement with the intermediate structures observed in the (γ,n) giant resonance. Unfortuantely their calculation did not extend above $E_x = 26$ MeV. It would now be interesting to see if the higher structures observed in $(^{3}He,\gamma)$ could be accommodated within the framework of this model.

    B. Capture to excited states

As mentioned in the introduction, Shay et al.[7] have measured the combined yield to the first four excited states of ^{16}O in the $^{13}C(^{3}He,\gamma)^{16}O$ reaction. The excitation function obtained shows a broad resonance
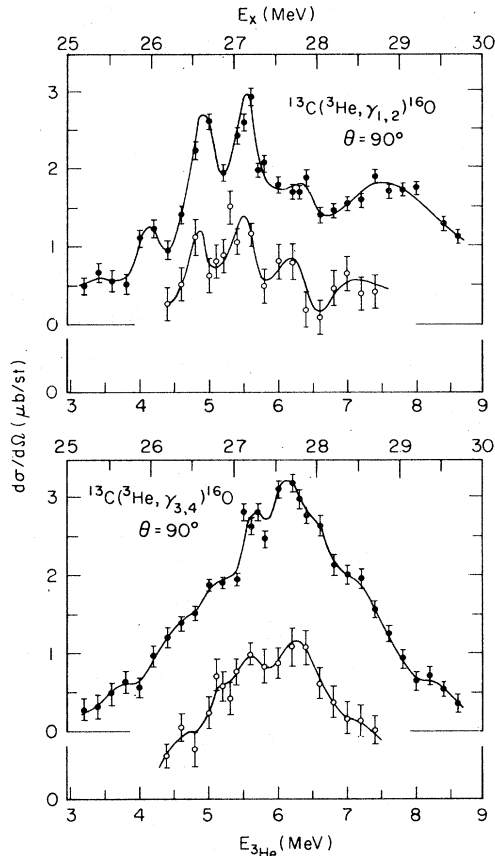
FIG. 7. Excitation functions of the differential cross sections for the reactions $^{13}C(^{3}He,\gamma_1+\gamma_2)^{16}O$ and $^{13}C(^{3}He,\gamma_3+\gamma_4)^{16}O$. Two independent runs are shown. Note that the open-circle data, although plotted to the same scale, have been shifted downward by a constant amount.

FIG. 8. Comparison between the $^{13}C(^{3}He,\gamma_1+\gamma_2)^{16}O$ and the $^{15}N(p,\gamma_1+\gamma_2)^{16}O$ (Ref. 12) capture reactions.

with little structure centered at approximately 27 MeV excitation energy in ^{16}O. In the present work, groups corresponding to the first (6.052 and 6.131 MeV) and second (6.917 and 7.119 MeV) doublets in ^{16}O were resolved. Figure 7 shows the 90° excitation functions for these two groups. Peaks in the $\gamma_1 + \gamma_2$ yield are observed at $E_x = 26.0 \pm 0.2$, 26.6 ± 0.2, 27.2 ± 0.2, 27.7 ± 0.2, and 28.6 ± 0.2 MeV, superposed on a broad giant-like structure. The differential cross section observed at the peak of the 26.2 MeV resonance is 3.0 ± 0.9 μb/sr. For the $\gamma_3 + \gamma_4$ transitions only mild structure is observed on a broad ($\simeq 2.5$ MeV wide) giant resonance centered at $E_x \simeq 27.5$ MeV. At the maximum, the differential cross section reaches a value of 3.2 ± 1.0 μb/sr.

Measurements of the $^{13}C(^{3}He,\gamma_1+\gamma_2)^{16}O$ and $^{13}C(^{3}He,\gamma_3+\gamma_4)^{16}O$ excitation functions at 90° in the energy range $E(^{3}He) = 4.0-7.5$ MeV have also been reported by Chew, Lowe, Nelson, and Barnett.[12] These authors report only the resonance at $E_x = 26.6$ MeV. Also, they measure a 90° differential cross
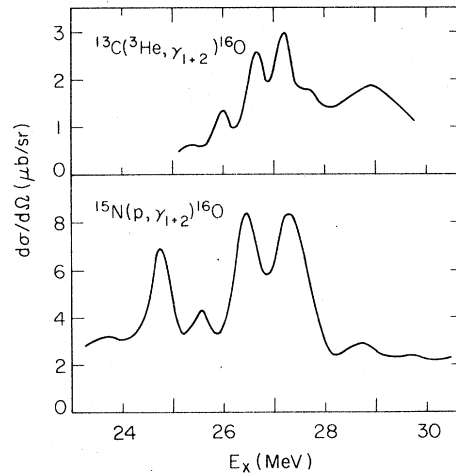
section that is a factor of two higher than the one reported here. This discrepancy in the differential cross section persists for the $^{13}C(^{3}He,\gamma_3+\gamma_4)$ reaction as well; however, in this case the shape of the yield curve is in fairly good agreement with the one reported here. In order to investigate the structure in these yield curves, they were run again and found to be in reasonable agreement with our earlier curves as shown in Fig. 7.

In a more recent measurement of the $^{13}C(^{3}He,\gamma_1+\gamma_2)$ excitation function at 0° the Birmingham group[13] did observe structure similar to that reported in this work at 90°. Thus, the existence of several resonances in the $^{13}C(^{3}He,\gamma_1+\gamma_2)$ excitation function appears to be confirmed.

The excitation region studied in this work with the $^{13}C(^{3}He,\gamma_1+\gamma_2)^{16}O$ capture reaction has also been investigated by Chew et al.[12] with the $^{15}N(p,\gamma_1+\gamma_2)^{16}O$ reaction. A comparison of the excitation functions is shown in Fig. 8. It is seen that the $(p,\gamma_1+\gamma_2)$ yield curve also exhibits considerable structure over this region and that there may be some correspondence between the peaks observed in the two reactions, especially if the threshold of the ^{3}He reaction is taken into account.

IV. CONCLUSION

Prominent E1 strength has been observed in the $^{13}C(^{3}He,\gamma_0)^{16}O$ capture reaction over the energy range $E_x = 24-30$ MeV in ^{16}O. The observed resonances at $E_x = 24.1$, 25.1, 26.0 and 27.3 MeV are postulated as being mainly 3p-3h states similar to those postulated by Shakin and Wang in their calculation of the GDR of ^{16}O. The measured angular distributions allow the reaction amplitudes to vary from almost pure $s_{1/2}$ wave to predominantly $d_{3/2}$ wave as the energy increases.

The excitation functions for the transitions to higher excited states in ^{16}O strongly indicate the presence of giant resonances built upon these states. The $^{13}C(^3He, \gamma_1 + \gamma_2)^{16}O$ yield curve shows resonances at $E_x = 26.0$, 26.6, 27.2, 27.7 and 28.6 MeV not previously reported in similar experiments. Structure is also observed in the $\gamma_3 + \gamma_4$ yield curves. These structures are similar in nature to that observed in the $(^3He, \gamma_0)$ reaction and in the $^{15}N(p, \gamma_0)^{16}O$ reaction.

---

*Present address: University of Maryland, College Park, Maryland 20742.
**Present address: 7301 Allan Ave., Falls Church, VA 22046.
[1]V. Gillet, M. A. Melkanoff, and J. Raynal, Nucl. Phys. A97, 631 (1967).
[2]M. Suffert, Nucl. Phys. 75, 226 (1966).
[3]J. R. Calarco, S. W. Wissink, M. Sasao, K. Wienhard, and S. S. Hanna, Phys. Rev. Lett. 39, 925 (1977).
[4]C. M. Shakin and W. L. Wang, Phys. Rev. Lett. 26, 902 (1971).
[5]N. G. Puttaswamy and D. Kohler, Phys. Lett. 20, 288 (1966).
[6]E. Ventura, C. C. Chang, E. M. Diener, S. S. Hanna, and G. A. Fisher, Bull. Am. Phys. Soc. 17, 113 (1972).
[7]H. D. Shay, R. E. Peschel, J. M. Long, and D. A. Bromley, Phys. Rev. C 9, 76 (1974).
[8]M. Suffert, W. Feldman, J. Mahieux, and S. S. Hanna, Nucl. Instrum. Methods 63, 1 (1968).
[9]S. L. Blatt, private communication.
[10]K. A. Snover, E. G. Adelberger, and D. R. Brown, Phys. Rev. Lett. 32, 1061 (1974).
[11]W. J. O'Connell and S. S. Hanna, Phys. Rev. C 17, 892 (1978).
[12]S. H. Chew, J. Lowe, J. M. Nelson, and A. R. Barnett, Nucl. Phys. A229, 241 (1974).
[13]J. Lowe, private communication.